International Journal of Aeronautical and Space Sciences (2018) 19:661–674
https://doi.org/10.1007/s42405-018-0076-5

IJASS International Journal of Aeronautical and Space Sciences

ORIGINAL PAPER

Robustness Improvement for a Three-Loop Missile Autopilot Using Discontinuous State Feedback

Donghyeok Hwang[1] · Min-Jea Tahk[1]

Received: 10 December 2017 / Revised: 6 February 2018 / Accepted: 6 February 2018 / Published online: 28 August 2018
© The Korean Society for Aeronautical & Space Sciences and Springer Nature Singapore Pte Ltd. 2018

Abstract
For several decades, the classical three-loop autopilot topologies have been successfully employed as missile longitudinal autopilots. To achieve robustness against matched and unmatched parametric uncertainties, this paper proposes two possible designs from a sliding mode control perspective. This paper first introduces what is termed a variable structure three-loop controller (VS3LC), which requires the same commanded and sensed quantities as the classical three-loop autopilot, but uses discontinuous feedback gains and an additional term for robustness improvement. It is found that the solution of this topology results in continuous equivalent control having the same expression as the classical three-loop autopilot when in sliding mode. Next, another variable structure pitch rate controller (VSPRC) which is insensitive to unmatched model parameter uncertainties as well as matched uncertainties is presented. The VSPRC combined with an additional outer-loop control of acceleration results in another three-loop topology, which is named as a variable structure-combined three-loop controller (VSC3LC). The robust performance and stability of the proposed variable structure controllers are illustrated through numerical simulations.

Keywords Sliding mode control · Three-loop autopilot · Robustness · Unmatched uncertainties

1 Introduction

Longitudinal autopilots for tactical missiles have been successfully employed for over 50 years, and the classical three-loop autopilot [1–3] has been successfully employed as the design topology of choice during the past several years. From a control point of view, however, modeling imprecision may come from actual uncertainty about the plant or from the purposeful choice of a simplified representation of the system's dynamics. Modeling inaccuracies can have strong adverse effects on control systems. Therefore, any practical design must address them explicitly.

To improve the robustness of the classical three-loop topology, a "neoclassic" four-loop autopilot which uses four gains instead of three has been presented [2]. In Ref. [2], the four-loop topology uses the same plant model as the three-loop autopilots except that an added first-order lag is explicitly taken into account using the additional gain. In Ref. [3], ten distinct topologies that use combinations of acceleration, angular rate, and first-order leads have been examined to determine the "best" from a robustness perspective. It has been shown that the classic topology typically has the best robustness properties. If there exists a large model mismatch between the model for design and the actual plant, the classical three-loop design itself does not assure effective control without exact modeling of the uncertainties or disturbance estimation.

An effective approach to robust control is so-called sliding control methodology. Due to the robustness of sliding mode with respect to model uncertainties or external disturbances, sliding mode control has been applied to practical systems, for example, autopilot design of agile missiles [4], autopilot design of aircraft [6], an integrated attitude and acceleration controller for skid-to-turn (STT) missiles [7], and autopilot for agile missiles and integrated guidance and control [8]. Higher order sliding mode control also has been used for the design of integrated attitude control using linearized attitude dynamics [5], aircraft pitch autopilots [9], integrated guidance and autopilot for dual controlled missiles [10] and missile guidance laws [11]. A major difficulty associated with the sliding mode method for missile acceleration

✉ Min-Jea Tahk
mjtahk@kaist.ac.kr

Donghyeok Hwang
dhhwang@add.re.kr

[1] Department of Aerospace Engineering, KAIST, Daejeon 34141, Republic of Korea

control comes from the fact that the dynamics which describe missile acceleration are non-minimum phase. To overcome this difficulty, a number of methods have been proposed. In references [15, 16], the plant inversion based on feedback linearization is first applied to the control of angle of attack. Normal acceleration is then controlled by the classical integral or proportional integral (PI) feedback. However, these methods have a weakness which can be unstable with respect to time delay. On the other hand, robust lateral acceleration autopilot [17] is designed for a tactical missile modeled as a second-order quasi-linear parameter varying system. In Ref. [17], the augmented lateral acceleration signal is used to overcome the effect of non-minimum phase. In Ref. [18], angle of attack is assumed as the known value, which is perfect, and is applied to the asymptotic output tracking control approach for angle of attack control.

In this paper, two simple but effective feasible designs from a sliding mode control perspective are proposed. First, the authors introduce what is termed a variable structure three-loop controller (VS3LC) to improve the robustness of the classical three-loop design against matched uncertainties. When sliding mode control laws are applied to the real missile system, how easily control law can be implemented is very important. One factor to be considered is what kind of information the designed control law requires and whether the required information can be easily obtained. The VS3LC law needs the same information as the classical three-loop design, but it requires discontinuous feedback gains instead of continuous feedback gains and an additional term for robustness improvement. The main advantage of the proposed scheme is that continuous equivalent control of the VS3LC has the same expression as the classical three-loop autopilot when in sliding mode.

Next, to deal with the unmatched parametric uncertainties which are related with the aerodynamic coefficients, we introduce another control law which is named as a variable structure-combined three-loop controller (VSC3LC). A state transformation that leads to the canonical subspace with respect to the pitch rate coordinate and its derivatives is derived to avoid the difficulty associated with the non-minimum phase dynamics of missile acceleration. Variable structure pitch rate controller (VSPRC), which is insensitive to unmatched as well as matched uncertainties, is derived with expression for uncertainties. The VSPRC combined with an additional outer-loop control results in the proposed VSC3LC which improves the robustness of the classical three-loop design against matched and unmatched uncertainties. The performance and robustness of the proposed controllers are illustrated by numerical simulations in the presence of uncertainties.

2 Preliminary Concepts

2.1 The Classical Three-Loop Autopilot Using State Feedback

In this section, the classical three-loop missile autopilot is designed in pitch plane using state feedback. The missile airframe dynamics are determined by six-dimensional equations of forces and moments acting on the missile body. The longitudinal missile dynamics, using the small disturbance linearization assumptions, are given as

$$\begin{aligned} \dot{\alpha} &= Z_1\alpha + q + Z_2\delta, \\ \dot{q} &= M_1\alpha + M_2\delta. \end{aligned} \tag{1}$$

The variable that is to be commanded is denoted as A_{L}, and modeled as

$$A_{\mathrm{L}} = -VZ_1\alpha - VZ_2\delta, \tag{2}$$

where α is the angle of attack, q is the pitch rate, V is the missile velocity, δ is the fin deflection, A_{L} is the missile normal acceleration, and Z_1, Z_2, M_1, and M_2 are the aerodynamics coefficients. The typical measurements available from the inertial measurement unit are normal acceleration A_{L} and pitch rate q. It is desirable to replace the angle of attack state in Eq. (1) with normal acceleration. Differentiating the expression for A_{L} and substituting from Eq. (1) yields:

$$\dot{A}_{\mathrm{L}} = -VZ_1(Z_1\alpha + q + Z_2\delta) - VZ_2\dot{\delta}. \tag{3}$$

Differentiating the expression for q and substituting from Eq. (1) yields:

$$\ddot{q} = M_1(Z_1\alpha + q + Z_2\delta) + M_2\dot{\delta}. \tag{4}$$

Modeling these linear dynamics in state space form yields the following pitch system state vector and control input.

$$\begin{bmatrix} \dot{A}_{\mathrm{L}} \\ \dot{q} \\ \ddot{q} \end{bmatrix} = \begin{bmatrix} Z_1 & -VZ_1 & 0 \\ 0 & 0 & 1 \\ -\frac{M_1}{V} & M_1 & 0 \end{bmatrix} \begin{bmatrix} A_{\mathrm{L}} \\ q \\ \dot{q} \end{bmatrix} + \begin{bmatrix} -VZ_2 \\ 0 \\ M_2 \end{bmatrix} \dot{\delta}. \tag{5}$$

The goal is to drive the commanded output A_{L} to track the normal acceleration command A_{LC} which is assumed constant, because in autopilot design we usually impose the requirement of tracking a step signal. In state feedback, the control law is composed of three state feedback gains as follows:

$$\dot{\delta} = k_4 A_{\mathrm{LC}} - \begin{bmatrix} k_1 & k_2 & k_3 \end{bmatrix} \begin{bmatrix} A_{\mathrm{L}} \\ q \\ \dot{q} \end{bmatrix}. \tag{6}$$

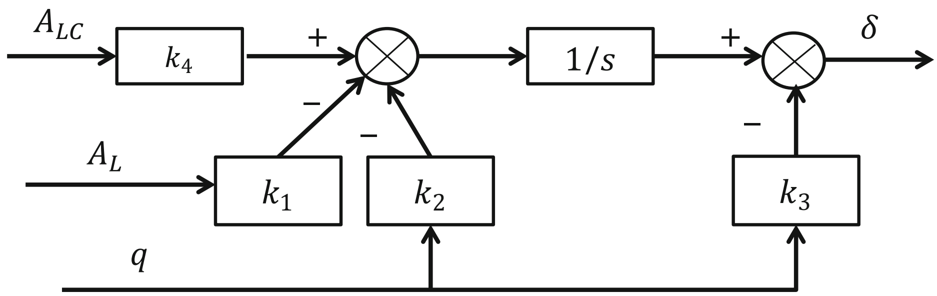

Fig. 1 Three-loop autopilot with state feedback

Notice that the control law applied to the real plant is actually not $\dot{\delta}$, but δ; so if we integrate both sides of Eq. (6), the fin control, δ, will be (assuming $\delta_0 = 0$ at the gain design point)

$$\delta = k_4 \int A_{LC} - k_1 \int A_L - k_2 \int q - k_3 q. \tag{7}$$

This formulation results in a kind of three-loop autopilot, which is presented in Fig. 1.

2.2 The Matched and Unmatched Uncertainties in Sliding Mode Control

Consider the following linear time invariant system:

$$\dot{x} = Ax + Bu, \tag{8}$$

where x and u are n- and m-dimensional state and control vectors, respectively, and A and B are constant matrices, $\mathrm{rank}(B) = m$. The system is assumed to be controllable. Because $\mathrm{rank}(B) = m$, matrix B in Eq. (8) may be partitioned (after re-ordering the state vector components) as

$$B = \begin{bmatrix} B_1 \\ B_2 \end{bmatrix}, \tag{9}$$

where $B_1 \in R^{(n-m)\times m}$ and $B_2 \in R^{m\times m}$. The nonsingular coordinate transformation,

$$T = \begin{bmatrix} I_{n-m} & -B_1 B_2^{-1} \\ 0 & B_2^{-1} \end{bmatrix}, \tag{10}$$

reduces the system Eqs. (8) and (9) to regular form,

$$\begin{bmatrix} \dot{x}_1 \\ \dot{x}_2 \end{bmatrix} = \begin{bmatrix} A_{11} & A_{12} \\ A_{21} & A_{22} \end{bmatrix} \begin{bmatrix} x_1 \\ x_2 \end{bmatrix} + \begin{bmatrix} 0 \\ u \end{bmatrix}, \tag{11}$$

where $x_1 \in R^{(n-m)}$, $x_2 \in R^m$. It follows from controllability of (A, B) that the pair (A_{11}, A_{12}) is controllable as well. However, in practical applications, the system in Eq. (8) operates under uncertainty conditions that may be generated by parametric variations ΔA and un-modeled dynamics $f(t)$. Under this condition, the real trajectory of the closed-loop control system may be summarized by

$$\dot{x} = (A + \Delta A)x + Bu + Qf(t), \tag{12}$$

where $f(t) \in R^l$ and Q is constant matrix. Sliding modes in any manifold are invariant with respect to parametric variations ΔA and un-modeled dynamics $f(t)$ if

$$\Delta A \in \mathrm{range}(B), \quad Q \in \mathrm{range}(B). \tag{13}$$

In other words, control u is assumed to be able to influence all components of the vector via control matrix B. When the uncertainty lies in the same channel as the input, then by varying the input, the effect of the uncertainty can be eliminated. In this case it is called a matched uncertainty. Otherwise, it is called an unmatched uncertainty.

3 The Variable Structure Three-Loop Controller (VS3LC)

3.1 Un-Modeled Dynamics

Consider a first-order lag into the flight control system that captures relevant un-modeled dynamics reflected to the input of the plant. In other words, let

$$\ddot{\delta} = -\frac{1}{T}\dot{\delta} + \frac{1}{T}\dot{\delta}_c, \tag{14}$$

where $\dot{\delta}$ is the fin rate, $\dot{\delta}_c$ is the fin rate command, and T is an uncertain delay but with known bounds $0 < T_{\min} \le T \le T_{\max}$. Now the state variables of the longitudinal missile dynamics are augmented with the fin rate $\dot{\delta}$, and the control is set to the fin rate command $\dot{\delta}_c$. The new state space representation is

$$\begin{bmatrix} \dot{A}_L \\ \dot{q} \\ \ddot{q} \\ \ddot{\delta} \end{bmatrix} = \begin{bmatrix} Z_1 & -VZ_1 & 0 & -VZ_2 \\ 0 & 0 & 1 & 0 \\ -\frac{M_1}{V} & M_1 & 0 & M_2 \\ 0 & 0 & 0 & -\frac{1}{T} \end{bmatrix} \begin{bmatrix} A_L \\ q \\ \dot{q} \\ \dot{\delta} \end{bmatrix} + \begin{bmatrix} 0 \\ 0 \\ 0 \\ \frac{1}{T} \end{bmatrix} \dot{\delta}_c. \tag{15}$$

3.2 Design of Sliding Mode Control Law with Discontinuous State Feedback

Let the sliding surface be

$$s = \begin{bmatrix} k_1 & k_2 & k_3 & 1 \end{bmatrix} \begin{bmatrix} A_L \\ q \\ \dot{q} \\ \dot{\delta} \end{bmatrix} - k_4 A_{\mathrm{LC}}, \tag{16}$$

where the $k_{1\text{–}4}$ coefficients are selected to achieve the characteristic required from the system when the state variables are in sliding mode. A_{LC} is the normal acceleration command, and A_{L} is commanded output. When in sliding mode, $s = 0$, thus Eq. (16) turns into Eq. (6) which describes the classical three-loop autopilot using state feedback.

The sliding surface in Eq. (16) has relative degree one because the first-time derivative of the sliding variables s is a function of control $\dot{\delta}_c$

$$\dot{s} = \sum_{i=1}^{3}\left(f_i + \frac{k_i}{T}\right)x_i + \sum_{i=4}^{5}\left(f_i - \frac{k_i}{T}\right)x_i + \frac{1}{T}\dot{\delta}_c, \tag{17}$$

where $x_1 = A_L,\ x_2 = q,\ x_3 = \dot{q},\ x_4 = A_{LC},\ x_5 = s$ and $k_5 = 1$.

$$\begin{aligned} f_1 &= k_1 Z_1 - \frac{k_3 M_1}{V} + k_1^2 V Z_2 - k_1 k_3 M_2, \\ f_2 &= -k_1 V Z_1 + k_3 M_1 + k_1 k_2 V Z_2 - k_2 k_3 M_2, \\ f_3 &= k_2 + k_1 k_3 V Z_2 - k_3^2 M_2, \\ f_4 &= -k_1 k_4 V Z_2 + k_3 k_4 M_2, \\ f_5 &= -k_1 V Z_2 + k_3 M_2. \end{aligned}$$

Once sliding mode is established, the state variables satisfy the condition of $\dot{s} = 0$, and the equivalent control is given by

$$\begin{aligned} \dot{\delta}_{c_{eq}} = &-\left(k_1 + \hat{T} f_1\right) A_{\mathrm{L}} - \left(k_2 + \hat{T} f_2\right) q \\ &- \left(k_3 + \hat{T} f_3\right) \dot{q} + \left(k_4 - \hat{T} f_4\right) A_{\mathrm{LC}}, \end{aligned} \tag{18}$$

where $\hat{T}$ is the estimate of the unknown delay T. Substituting $\dot{\delta}_{c_{\mathrm{eq}}}$ into Eq. (15) yields the sliding mode equation as

$$\begin{aligned} \begin{bmatrix} \dot{A}_L \\ \dot{q} \\ \ddot{q} \end{bmatrix} &= \begin{bmatrix} Z_1 + k_1 V Z_2 & -V Z_1 + k_2 V Z_2 & k_3 V Z_2 \\ 0 & 0 & 1 \\ -\frac{M_1}{V} - k_1 M_2 & M_1 - k_2 M_2 & -k_3 M_2 \end{bmatrix} \begin{bmatrix} A_L \\ q \\ \dot{q} \end{bmatrix} \\ &+ \begin{bmatrix} -V Z_2 \\ 0 \\ M_2 \end{bmatrix} k_4 A_{\mathrm{LC}}. \end{aligned} \tag{19}$$

It is evident from Eq. (19) that once sliding mode is established, the uncertain delay T is rejected from the sliding mode equation, and the flight control system becomes invariant to the effect of the uncertain delay. The sliding surface gains $k_{1\text{–}4}$ must be chosen to satisfy some designer-chosen criteria. A useful gain selection methodology in classical three-loop design is to choose the open-loop crossover frequency so that many stability problems can be avoided. Usually, the crossover frequency is chosen to be no more than one-third of the bandwidth of the actuator to ensure a well-behaved flight control system response [13]. The closed-loop transfer function from A_{LC} to A_{L} is

$$G_{\mathrm{cl}}(s) = -k_4 \frac{V Z_2 s^2 + V(Z_1 M_2 - Z_2 M_1)}{s^3 + A_1 s^2 + A_2 s + A_3}, \tag{20}$$

where

$$\begin{aligned} A_1 &= -k_1 V Z_2 + k_3 M_2 - Z_1, \\ A_2 &= k_2 M_2 - k_3(Z_1 M_2 - Z_2 M_1) - M_1, \\ A_3 &= -(k_2 + k_1 V)(Z_1 M_2 - Z_2 M_1). \end{aligned}$$

The open-loop transfer function of the three-loop design can be expressed as

$$G_{\mathrm{op}}(s) = \frac{(A_1 + Z_1)s^2 + (A_2 + M_1)s + A_3}{s\left(s^2 - Z_1 s - M_1\right)}. \tag{21}$$

If we assume that the open-loop crossover frequency is beyond the airframe dynamics, we can say

$$\left|G_{\mathrm{op}}(j\omega_{cr})\right| = \frac{(k_3 M_2 - k_1 V Z_2)\omega_{\mathrm{cr}}^2}{\omega_{\mathrm{cr}}^3} \approx 1. \tag{22}$$

Solving for the crossover frequency yields

$$\omega_{\mathrm{cr}} = k_3 M_2 - k_1 V Z_2. \tag{23}$$

For a third-order flight control system, the desired closed-loop characteristic polynomial can be described by the three positive parameters τ, ζ_d, and ω_d in the following form:

$$d(s) = \left(s + \frac{1}{\tau}\right)\left(s^2 + 2\zeta_d\omega_d s + \omega_d^2\right), \tag{24}$$

where τ is desired time constant, ζ_d is desired damping ratio, and ω_d represents the desired natural frequency of the system. The positive selection of the three parameters guarantees the stability of the closed-loop. Moreover, the autopilot performance is totally described by these design parameters. By equating both characteristic equations, Eqs. (20) and (24), an analytical formula between the gains and design parameters is derived as follows:

$$\begin{aligned} 2\zeta_d\omega_d + \frac{1}{\tau} &= -k_1 V Z_2 + k_3 M_2 - Z_1, \\ \omega_d^2 + \frac{2\zeta_d\omega_d}{\tau} &= k_2 M_2 - k_3(Z_1 M_2 - Z_2 M_1) - M_1, \\ \frac{\omega_d^2}{\tau} &= -(k_2 + k_1 V)(Z_1 M_2 - Z_2 M_1). \end{aligned} \tag{25}$$

In addition, we have already derived an expression for the open-loop crossover frequency in Eq. (23). If we specify the desired time constant, damping ratio and open-loop crossover frequency of the flight control system, we can solve the four unknowns, $k_{1\text{–}3}$ and ω_d, as follows:

$$\omega_d = \frac{\omega_{cr} - \frac{1}{\tau} - Z_1}{2\zeta_d} \tag{26}$$

and

$$\begin{bmatrix} k_1 \\ k_2 \\ k_3 \end{bmatrix} = \begin{bmatrix} -VZ_2 & 0 & Z_2 \\ 0 & M_2 & Z_2 M_1 - Z_1 M_2 \\ V & 1 & 0 \end{bmatrix}^{-1} \begin{bmatrix} 2\zeta_d\omega_d + \frac{1}{\tau} + Z_1 \\ \omega_d^2 + \frac{2\zeta_d\omega_d}{\tau} + M_1 \\ \frac{\omega_d^2}{\tau(Z_2 M_1 - Z_1 M_2)} \end{bmatrix}. \tag{27}$$

From Eqs. (26) and (27), the state feedback gains $k_{1\sim3}$ are described in terms of the design parameters τ, ζ_d, and ω_{cr}. Finally, to get unity flight control system gain, we set the gain of the closed-loop transfer function to unity and get

$$k_4 = \frac{k_2 + k_1 V}{V}. \tag{28}$$

Based on Eqs. (26)–(28), the autopilot design is handled by the desired time constant, damping ratio, and open-loop crossover frequency to achieve the desired performance requirements.

Now, the control law enforcing sliding mode in the surface $s = 0$ is examined. The control law of the following form is considered.

$$\dot{\delta}_c = -\psi_1 A_L - \psi_2 q - \psi_3 \dot{q} + \psi_4 A_{LC} + \psi_5 s, \tag{29}$$

where $\psi_{1\text{–}3}$ are the discontinuous state feedback gains to be determined. The additional term $\psi_5 s$ is included for robustness improvement. The Lyapunov function is chosen as $L = \frac{1}{2}s^2$, which implies $\dot{L} = s\dot{s}$. The existence condition for sliding mode is fulfilled if

$$s\dot{s} = \sum_{i=1}^{3}\left(f_i + \frac{k_i - \psi_i}{T}\right)x_i s + \sum_{i=4}^{5}\left(f_i - \frac{k_i - \psi_i}{T}\right)x_i s < 0. \tag{30}$$

The following result gives a condition for the discontinuous gains $\psi_{1\sim5}$ to make the system stable.

Theorem 1 *The autopilot system in Eq. (29) will be stable if the following conditions are met*

$$\psi_i = \begin{cases} k_i + g\hat{T} f_i, & f_i x_i s > 0 \\ k_i, & f_i x_i s = 0\,, \\ k_i - g\hat{T} f_i, & f_i x_i s < 0 \end{cases} \quad \textit{for } i = 1, 2, 3,$$
$$\psi_i = \begin{cases} k_i - g\hat{T} f_i, & f_i x_i s > 0 \\ k_i, & f_i x_i s = 0\,, \\ k_i + g\hat{T} f_i, & f_i x_i s < 0 \end{cases} \quad \textit{for } i = 4, 5, \tag{31}$$

where the estimate $\hat{T}$ of the delay T is taken as the geometric mean of the known bounds, $0 < T_{min} \le T \le T_{max}$,

$$\hat{T} = \sqrt{T_{max} T_{min}} \tag{32}$$

and $g \ge \sqrt{T_{max}/T_{min}}$ is constant for all time.

Proof If $\psi_{i=1\text{–}3}$ are chosen as $k_i \pm g\hat{T} f_i$ in accordance with the sign of $f_i x_i s$, then

$$\left(f_i + \frac{k_i - \psi_i}{T}\right)x_i s = f_i x_i s - \frac{g\hat{T}}{T}|f_i x_i s|, \quad \text{for } i = 1, 2, 3 \tag{33}$$

and if $\psi_{i=4,5}$ are chosen as $k_i \mp g\hat{T} f_i$ according to the sign of $f_i x_i s$, then

$$\left(f_i - \frac{k_i - \psi_i}{T}\right)x_i s = f_i x_i s - \frac{g\hat{T}}{T}|f_i x_i s|, \quad \text{for } i = 4, 5. \tag{34}$$

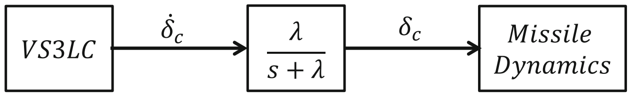

Fig. 2 Block diagram of a smooth control law for VS3LC

The constant g is defined as $\geq \sqrt{T_{max}/T_{min}}$, so the following inequality holds

$$0 < g^{-1} \leq \frac{\hat{T}}{T} \leq g. \tag{35}$$

Thus, if $\psi_{i=1\text{–}5}$ are chosen as Eqs. (30) and (31), the control law of Eq. (29) ensures

$$s\dot{s} = \sum_{i=1}^{3}\left(f_i + \frac{k_i - \psi_i}{T}\right)x_i s + \sum_{i=4}^{5}\left(f_i - \frac{k_i - \psi_i}{T}\right)x_i s < 0. \tag{36}$$

From the definition of L, s converges to zero.

Notice that the control law applied to the real plant is actually not $\dot{\delta}_c$, but δ_c; so a smooth control law for VS3LC is obtained by low pass filtering $\dot{\delta}_c$ [14]. Although the $\dot{\delta}_c$ shows chattering phenomenon because of a switching function, the δ_c applied to the real plant does not show the chattering phenomenon. Figure 2 shows the overall block diagram of the proposed method.

4 The Variable Structure Pitch Rate Controller (VSPRC)

4.1 Model Uncertainties

The aerodynamic coefficients described by Z_1, Z_2, M_1, and M_2 are dependent on Mach number and angle of attack. These parameters are usually measured from wind tunnel tests, and these values may contain some error when compared with true values because of the imperfection of the measurements. These errors are assumed to be bounded and can be modeled as multiplicative uncertainties

$$Z_i^{\text{pert}} = (1 \pm \Delta_i)Z_i,$$
$$M_i^{\text{pert}} = (1 \pm \Delta_i)M_i. \tag{37}$$

where Z_i and M_i are the true aerodynamic coefficients, Z_i^{pert} and M_i^{pert} are the measured aerodynamic coefficients, and Δ_{i} represents the admissible uncertainties, and its maximum value is about 0.2–0.5. Hence the longitudinal missile dynamic model, using the small disturbance linearization assumption, can be represented in state space form as follows:

$$\begin{bmatrix} \dot{A}_L \\ \dot{q} \\ \ddot{q} \\ \dot{\delta} \end{bmatrix} = \begin{bmatrix} \hat{Z}_1 & -V\hat{Z}_1 & 0 & -V\hat{Z}_2 \\ 0 & 0 & 1 & 0 \\ -\frac{\hat{M}_1}{V} & \hat{M}_1 & 0 & \hat{M}_2 \\ 0 & 0 & 0 & -\frac{1}{\hat{T}} \end{bmatrix} \begin{bmatrix} A_L \\ q \\ \dot{q} \\ \delta \end{bmatrix} + \begin{bmatrix} 0 \\ 0 \\ 0 \\ \frac{1}{\hat{T}} \end{bmatrix} \dot{\delta}_c, \tag{38}$$

where Z_1, Z_2, M_1, M_2, and T are estimated as $\hat{Z}_1, \hat{Z}_2, \hat{M}_1, \hat{M}_2$, and $\hat{T}$. Note that all the uncertainties described in Eq. (38) are not matched with the control action, so any selection of sliding surface cannot decouple the parametric uncertainties from the state space representation. Therefore, a special mathematical method will need to be developed to determine conditions for sliding mode to be invariant to the unmatched uncertainties.

4.2 State Transformation into the Canonical Space

Sliding motion in any sliding surface could be invariant to external disturbances and parametric perturbation if the uncertainties act in a control space. The choice of a canonical space is due to the fact that the desired control could be attained even if they do not act in a control space in the original state representation [12]. To design an invariant sliding surface for a flight control system, it would be reasonable to consider autopilot design in the acceleration canonical space. However, to avoid the difficulty associated with the non-minimum phase dynamics of missile acceleration, we consider a state transformation that leads to a canonical space with respect to the pitch rate coordinate and its derivatives. Consider the transfer function from a fin deflection δ_c to missile pitch rate q:

$$q = \frac{M_2 s + Z_2 M_1 - Z_1 M_2}{(Ts+1)(s^2 - Z_1 s - M_1)}\delta_c. \tag{39}$$

The input δ_c and output q are related by a linear coefficient differential equation of the form:

$$\dddot{q} = \left(Z_1 - \frac{1}{T}\right)\ddot{q} + \left(M_1 + \frac{Z_1}{T}\right)\dot{q} + \frac{M_1}{T}q + \frac{M_2}{T}\dot{\delta}_c + \frac{Z_2 M_1 - Z_1 M_2}{T}\delta_c. \tag{40}$$

Equation (40) contains the derivative of control action δ_c. To realize invariant sliding mode, the control should be chosen so as to have a sliding surface s with a sign opposite to the sign of rate $\dot{s}$ that has first order discontinuous on the surface. This condition is satisfied if output of the dynamics

$$M_2\dot{\delta}_c + (Z_2 M_1 - Z_1 M_2)\delta_c = v \tag{41}$$

is used as the control, where v is the discontinuous function of $q, \dot{q}$, and $\ddot{q}$. Let us define

$$q_1 = q, \quad q_2 = \dot{q}, \quad q_3 = \ddot{q}. \tag{42}$$

If v is considered to be control action, we can then represent Eq. (40) with new state variables in pitch rate canonical subspace as follows:

$$\begin{bmatrix} \dot{q}_1 \\ \dot{q}_2 \\ \dot{q}_3 \\ \dot{\delta}_c \end{bmatrix} = \begin{bmatrix} 0 & 1 & 0 & 0 \\ 0 & 0 & 1 & 0 \\ \frac{M_1}{T} & M_1 + \frac{Z_1}{T} & Z_1 - \frac{1}{T} & 0 \\ 0 & 0 & 0 & \frac{Z_1 M_2 - Z_2 M_1}{M_2} \end{bmatrix} \begin{bmatrix} q_1 \\ q_2 \\ q_3 \\ \delta_c \end{bmatrix} + \begin{bmatrix} 0 \\ 0 \\ \frac{1}{T} \\ \frac{1}{M_2} \end{bmatrix} v, \tag{43}$$

where $q(= q_1)$ is the controlled variable. The goal is to drive the commanded output q to track the pitch rate command q_c which is assumed constant.

4.3 Design of the Variable Controller with Discontinuous State Feedback

Let the sliding surface be selected in pitch rate canonical subspace

$$s = c_1 q_1 + c_2 q_2 + q_3 - c_3 q_c, \tag{44}$$

where q_c is the pitch rate command, q_1, q_2, q_3 are defined in Eq. (42), and the c_{1-3} coefficients are selected to achieve the characteristics required from the system when the state variables are in sliding mode. This choice of the sliding surface is due to the fact that the sliding mode in the canonical subspace can be invariant to parametric perturbations. It should be noted that the sliding surface is a function of three states only. Therefore, the control algorithm based on the knowledge of this sliding surface will be a partial state feedback law rather than a full state feedback law. Thus, it should be checked whether the state space model in Eq. (43) is asymptotically stable or not. The derivative of the sliding variables s is a function of control v

$$\dot{s} = \sum_{i=1}^{2}\left(h_i + \frac{c_i}{T}\right)x_i + \sum_{i=3}^{4}\left(h_i - \frac{c_i}{T}\right)x_i + \frac{1}{T}v, \tag{45}$$

where $x_1 = q, \; x_2 = \dot{q}, \; x_3 = q_c, \; x_4 = s$, and $c_4 = 1$.

$$h_1 = \frac{M_1}{T} - c_1 c_2 - c_1 Z_1,$$
$$h_2 = c_1 + M_1 + \frac{Z_1}{T} - c_2^2 - c_2 Z_1,$$
$$h_3 = c_1 c_2 + c_1 Z_1,$$
$$h_4 = c_2 + Z_1.$$

Once sliding mode is established, the state variables satisfy the condition of $\dot{s} = 0$ and the equivalent control is given by

$$v_{eq} = -\left(c_1 + \hat{T}\hat{h}_1\right)q_1 - \left(c_2 + \hat{T}\hat{h}_2\right)q_2 + \left(c_3 - \hat{T}\hat{h}_3\right)q_c, \tag{46}$$

where $\hat{h}_1, \hat{h}_2, \hat{h}_3$ and $\hat{T}$ are estimates of the model parameters h_1, h_2, h_3 and unknown delay T. Substituting v_{eq} into Eq. (43) yields the sliding mode equations as

$$\begin{bmatrix} \dot{q}_1 \\ \dot{q}_2 \end{bmatrix} = \begin{bmatrix} 0 & 1 \\ -c_1 & -c_2 \end{bmatrix} \begin{bmatrix} q_1 \\ q_2 \end{bmatrix} + \begin{bmatrix} 0 \\ c_3 \end{bmatrix} q_c. \tag{47}$$

It is evident from Eq. (47) that once sliding mode is established, the parametric uncertainties $\hat{h}_1, \hat{h}_2, \hat{h}_3$, and unknown delay $\hat{T}$ are rejected from the sliding mode equations, so the flight control system becomes invariant to the effect of the uncertainties. The sliding surface gains c_{1-2} are chosen to satisfy some designer-chosen criteria. From Eq. (47), the closed-loop transfer function from q_c to q is

$$G_{cl} = \frac{c_3}{s^2 + c_2 s + c_1}. \tag{48}$$

For a second-order closed control system, the desired closed-loop characteristic polynomial can be described by the two parameters τ and ζ_d in the following form:

$$d(s) = s^2 + \frac{2}{\tau}s + \frac{1}{\tau^2 \zeta_d^2}, \tag{49}$$

where τ is desired time constant, and ζ_d is desired damping ratio. The control performance is totally described by these design parameters. By comparing both characteristic polynomials, Eqs. (48) and (49), relations between the gains and design parameters are derived as follows:

$$c_2 = \frac{2}{\tau},$$
$$c_1 = c_3 = \frac{1}{\tau^2 \zeta^2}. \tag{50}$$

Based on Eq. (50), the sliding surface gains are handled by the desired time constant and damping ratio to achieve the desired performance requirements.

Next, the control law enforcing the sliding mode in the surface $s = 0$ is examined. The control law of the following form is considered

$$v = -\psi_1 q_1 - \psi_2 q_2 + \psi_3 q_c + \psi_4 s, \tag{51}$$

where $\psi_{1\text{–}2}$ are the discontinuous state feedback gains to be determined. The additional term $\psi_4 s$ is included for robustness improvement. The Lyapunov function is chosen as $L = \frac{1}{2}s^2$. The existence condition for sliding mode is fulfilled if

$$s\dot{s} = \sum_{i=1}^{2}\left(h_i + \frac{c_i - \psi_i}{T}\right)x_i s + \sum_{i=3}^{4}\left(h_i - \frac{c_i - \psi_i}{T}\right)x_i s < 0, \tag{52}$$

where $x_1 = q_1, x_2 = q_2, x_3 = q_c, x_4 = s$, and $c_4 = 1$. The following result gives a condition for the discontinuous gains $\psi_{1\text{–}4}$ to make the system stable.

Theorem 2 *The autopilot system in Eq. (51) will be stable if the following conditions are met.*

$$\psi_i = \begin{cases} c_i + \hat{T}\hat{h}_i + \hat{T}g_i, & x_i s > 0 \\ c_i + \hat{T}\hat{h}_i, & x_i s = 0\,, \quad \textit{for } i = 1, 2, \\ c_i + \hat{T}\hat{h}_i - \hat{T}g_i, & x_i s < 0 \end{cases}$$
$$\psi_i = \begin{cases} c_i - \hat{T}\hat{h}_i - \hat{T}g_i, & x_i s > 0 \\ c_i - \hat{T}\hat{h}_i, & x_i s = 0\,, \quad \textit{for } i = 3, 4, \\ c_i - \hat{T}h_i - \hat{T}g_i, & x_i s < 0 \end{cases} \tag{53}$$

with

$$g_i \geq gH_i + |g - 1|\left|\hat{h}_i\right|, \quad \textit{for } i = 1, 2, 3, 4 \tag{54}$$

where the estimate $\hat{T}$ of the delay T is taken as the geometric mean of the known bounds, $0 < T_{min} \leq T \leq T_{max}$,

$$\hat{T} = \sqrt{T_{max}T_{min}}. \tag{55}$$

The $\hat{h}_i$ of the parameter h_i is taken so that the estimation error on h_i should be bounded by some known value H_i,

$$\left|h_i - \hat{h}_i\right| \leq H_i \tag{56}$$

and $g \geq \sqrt{T_{max}/T_{min}}$ is constant for all time.

Proof If $\psi_{i=1,2}$ are chosen as $c_i + \hat{T}\hat{h}_i \pm \hat{T}g_i$ in accordance with the sign of $x_i s$, then

$$\left(h_i + \frac{c_i - \psi_i}{T}\right)x_i s = \left(h_i - \frac{\hat{T}\hat{f}_i}{T}\right)x_i s - \frac{g_i\hat{T}}{T}|x_i s|, \quad \text{for } i = 1, 2. \tag{57}$$

If $\psi_{i=3,4}$ are also chosen as $c_i - \hat{T}\hat{h}_i \mp \hat{T}g_i$ according to the sign of $x_i s$, then

$$\left(h_i - \frac{c_i - \psi_i}{T}\right)x_i s = \left(h_i - \frac{\hat{T}\hat{f}_i}{T}\right)x_i s - \frac{g_i\hat{T}}{T}|x_i s|, \quad \text{for } i = 3, 4. \tag{58}$$

Since $h_i = \hat{h}_i + (h_i - \hat{h}_i)$, where $\left|h_i - \hat{h}_i\right| \leq H_i$, this in turn leads to

$$\left(h_i - \frac{\hat{T}\hat{f}_i}{T}\right)x_i s - \frac{g_i\hat{T}}{T}|x_i s| \leq \left(H_i + \hat{h}_i - \frac{\hat{T}\hat{h}_i}{T}\right)x_i s - \frac{g_i\hat{T}}{T}|x_i s|. \tag{59}$$

Thus, by choosing g_i to be large enough

$$g_i \geq gH_i + |g - 1|\left|\hat{h}_i\right| \geq \frac{T}{\hat{T}}H_i + \left|\frac{T}{\hat{T}} - 1\right|\left|\hat{h}_i\right|. \tag{60}$$

We can guarantee that

$$s\dot{s} = \sum_{i=1}^{2}\left(h_i + \frac{c_i - \psi_i}{T}\right)x_i s + \sum_{i=3}^{4}\left(h_i - \frac{c_i - \psi_i}{T}\right)x_i s < 0. \tag{61}$$

From the definition of L, s converges to zero.

Fig. 3 The structure of VSC3LC

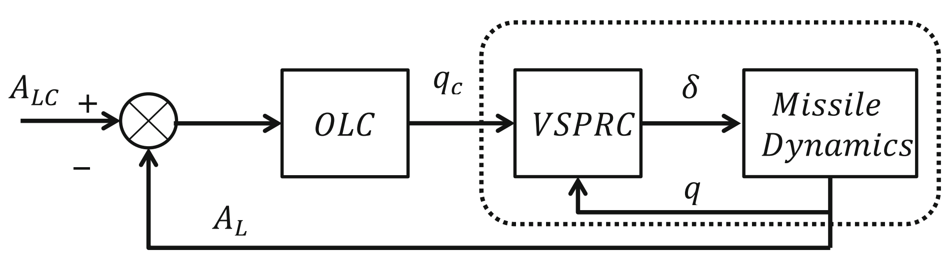

Table 1 Missile parameters

Variable	Value	Units	Description
V_M	914	m/s	Missile velocity
m	453	kg	Missile mass
I_{yy}	1407	kg m^2	Pitch moment of inertia
C_{N_α}	32.5928	–	Pitch force coefficient due to angle of attack
C_{M_α}	− 79.2582	–	Pitch moment coefficient due to angle of attack
C_{N_δ}	7.2025	–	Pitch force coefficient due to fin deflection
C_{M_δ}	− 68.4239	–	Pitch moment coefficient due to fin deflection
Q	511,990	kg /ms^2	Dynamic pressure
S	0.073	m^2	Reference area
d	0.3	m	Reference length
Z_1	− 2.9356	s^{-1}	Aerodynamics coefficient
Z_2	− 0.6487	s^{-1}	Aerodynamics coefficient
M_1	− 641.2892	s^{-2}	Aerodynamics coefficient
M_2	− 553.6272	s^{-2}	Aerodynamics coefficient

5 The Variable Structure-Combined Three-Loop Controller (VSC3LC)

In the previous section, the variable structure pitch rate controller (VSPRC) has been designed to track pitch rate reference in spite of the existence of model unmatched uncertainties. However, the objective of this study is to track the reference acceleration. Hence, a cascaded control structure is introduced, as shown in Fig. 3, where VSPRC is augmented by an outer-loop controller (OLC) to control the acceleration. The outer-loop controller is defined as

$$q_c = \left(\frac{k_2}{s + k_1}\right)(k_3 A_{\mathrm{LC}} - A_{\mathrm{L}}), \tag{62}$$

where the coefficients $k_{1\text{–}3}$ are the outer-loop controller gains to be chosen such that the closed-loop satisfies performance requirements. Once sliding mode is established, the transfer function from q_c to q simplifies to

$$\frac{q}{q_c} = \frac{c_1}{s^2 + c_2 s + c_1}, \tag{63}$$

where the gains $c_{1\text{–}2}$ determine the characteristics of VSPRC.

Also, if we assume steady-state condition, A_{L} can be related by q as

$$A_{\mathrm{L}} = Vq. \tag{64}$$

By substituting Eqs. (62) and (63) into Eq. (64), the closed-loop transfer function from A_{LC} to A_{L} is obtained,

$$G_{\mathrm{cl}}(s) = \frac{Vk_2k_3c_1}{s^3 + (c_2 + k_1)s^2 + (c_1 + k_1c_2)s + k_1c_1 + Vk_2c_1}, \tag{65}$$

and open-loop transfer function can be expressed as

$$G_{\mathrm{op}}(s) = \frac{k_1s^2 + k_1c_2s + k_1c_1 + Vk_2c_1}{s^3 + c_2s^2 + c_1s}. \tag{66}$$

If we assume the open-loop crossover frequency is beyond the airframe dynamics, the crossover frequency can be approximated as

$$\omega_{\mathrm{cr}} = k_1. \tag{67}$$

Also, if we consider the desired closed-loop characteristics as

$$d(s) = \left(s + \frac{1}{\tau}\right)\left(s^2 + 2\zeta_d\omega_d s + \omega_d^2\right) \tag{68}$$

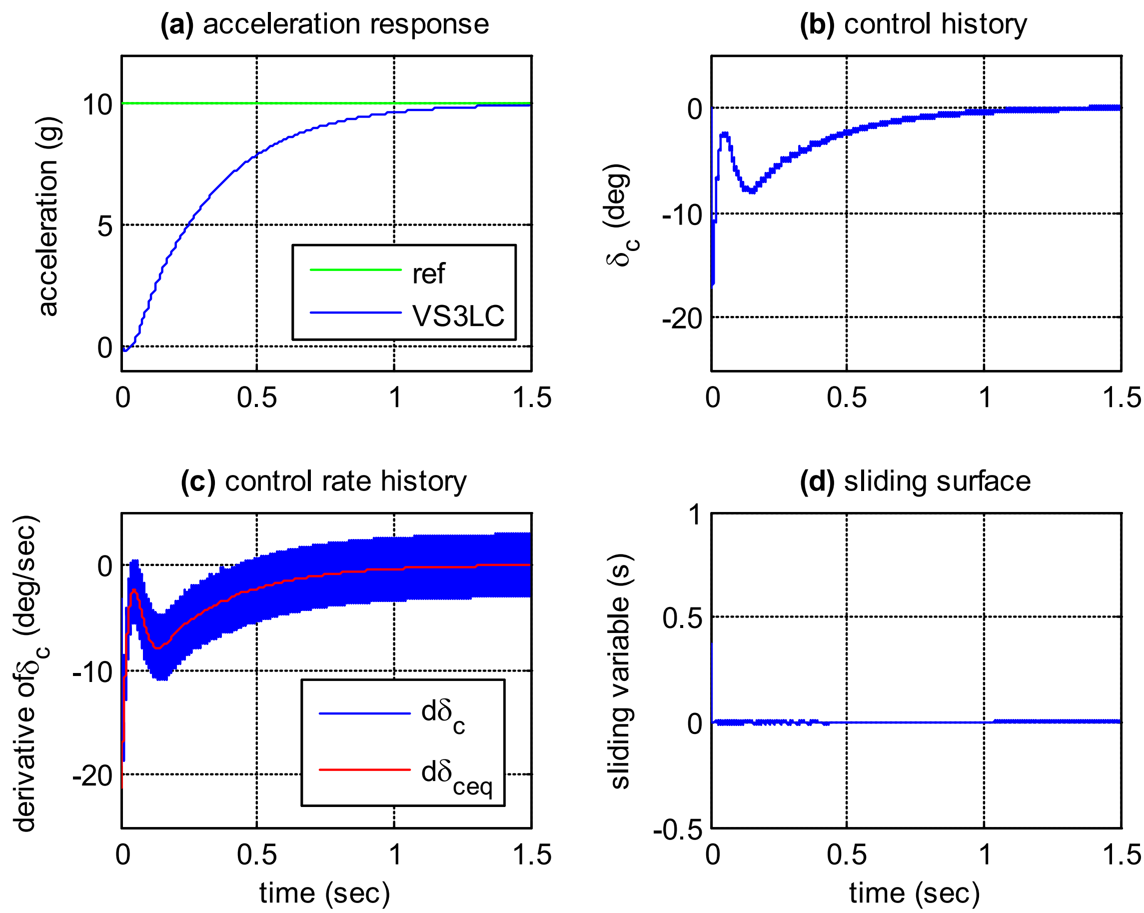

Fig. 4 Responses of VS3LC with unknown delay

Then controller gains are determined as

$$\begin{aligned} c_2 &= \frac{2}{\tau}, \\ c_1 &= \omega_d^2 + \frac{2\zeta_d\omega_d}{\tau} - c_2\omega_{cr}, \\ \omega_d &= \frac{c_2 + \omega_{cr} - \frac{1}{\tau}}{2\zeta_d}, \\ k_2 &= \frac{\omega_d^2}{Vc_1\tau} - \frac{k_1}{V}. \end{aligned} \tag{69}$$

Based on Eqs. (67)–(69), the gain design of VSC3LC is handled by the desired time constant, damping ratio, and open-loop crossover frequency to achieve the desired performance requirements.

6 Simulation Results

In this section, numerical simulation for VS3LC and VSC3LC with and without uncertainty is performed to demonstrate the effectiveness and robustness of the proposed variable controllers for the design goals which are to achieve a time constant of 0.3 s, open-loop crossover frequency of 50 rad/s, and a damping of 0.7. Table 1 summarizes the various missile parameters used in the examples.

Figures 4 and 5 show the responses generated by VS3LC. The switching hyper-plane used is

$$s = \begin{bmatrix} -0.0007 & -1.2012 & -0.0928 & 1 \end{bmatrix} \begin{bmatrix} A_L \\ q \\ \dot{q} \\ \dot{\delta} \end{bmatrix} + 0.0012A_{LC}, \tag{70}$$

where the sliding surface gains have been obtained to achieve the design goals based on Eqs. (26)–(28). Figure 4 shows the corresponding step response, control rate $\dot{\delta}_c$, equivalent control rate $\dot{\delta}_{c_{eq}}$ and control command signal δ_c, and sliding surface variable for a command $A_{LC} = 10\ g$, and using $T_{\max} = 1.5$ ms and $T_{\min} = 0.5$ ms. The estimate of T is 0.87, and a value of 1.7321 has been used for the upper limit of g. Although the $\dot{\delta}_c$ shows chattering phenomenon because of a switching function, the δ_c applied to the real plant does not show the chattering phenomenon.

Figure 5 compares the robustness of VS3LC with the classical three-loop design with respect to four different unknown

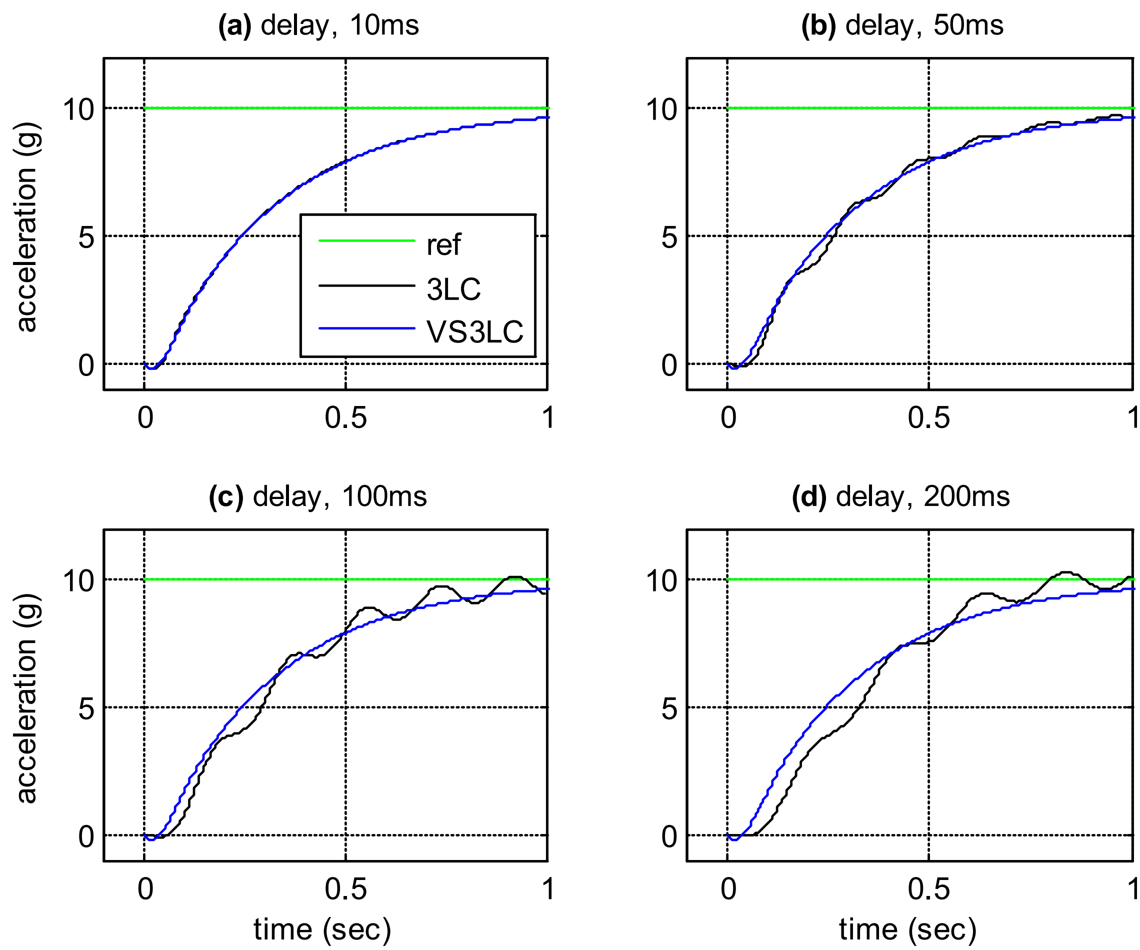

Fig. 5 Comparison of VS3LC and 3LC

delays $T = 10\,\text{ms},\ 50\,\text{ms},\ 100\,\text{ms}$, and 200 ms. The classical three-loop controller (3LC) starts to suffer badly as the unknown delay approaches the bandwidth of the system. The uncertainty deteriorates some of the robustness in the three-loop design and this effect gets worse as the delay gets longer. However, the responses of VS3LC kept insensitive to the uncertainty once sliding mode is established.

The performance of VSPRC and VSC3LC is examined in Fig. 6. The following representation of the longitudinal missile dynamics is considered,

$$\begin{bmatrix} \dot{q}_1 \\ \dot{q}_2 \\ \dot{q}_3 \\ \dot{\delta}_c \end{bmatrix} = \begin{bmatrix} 0 & 1 & 0 & 0 \\ 0 & 0 & 1 & 0 \\ -32113 & -789.26 & -52.93 & 0 \\ 0 & 0 & 0 & -2.18 \end{bmatrix} \begin{bmatrix} q_1 \\ q_2 \\ q_3 \\ \delta_c \end{bmatrix} + \begin{bmatrix} 0 \\ 0 \\ 50 \\ -0.0018 \end{bmatrix} v, \tag{71}$$

which has been obtained by a canonical state transformation. The switching hyper-plane used is

$$s = \begin{bmatrix} 22.6757 & 6.6667 & 1 & 0 \end{bmatrix} \begin{bmatrix} q_1 \\ q_2 \\ q_3 \\ \delta_c \end{bmatrix} - 22.6757 q_c, \tag{72}$$

Note that the control based on the knowledge of this sliding surface is a partial state feedback law rather than a full state feedback law. Therefore, it should be checked whether the state space model in Eq. (71) is asymptotically stable or not. The asymptotic stability of general motion in the system of Eq. (71) (rather than of motion in the canonical subspace only) is defined by the eigenvalues of the characteristic equation of Eq. (71). Figure 6 shows the corresponding step response, control signal, and sliding surface variable for a command $A_{LC} = 10\ g$. The estimate of T is 0.87, and the admissible uncertainties are set to 30% of the true aero-

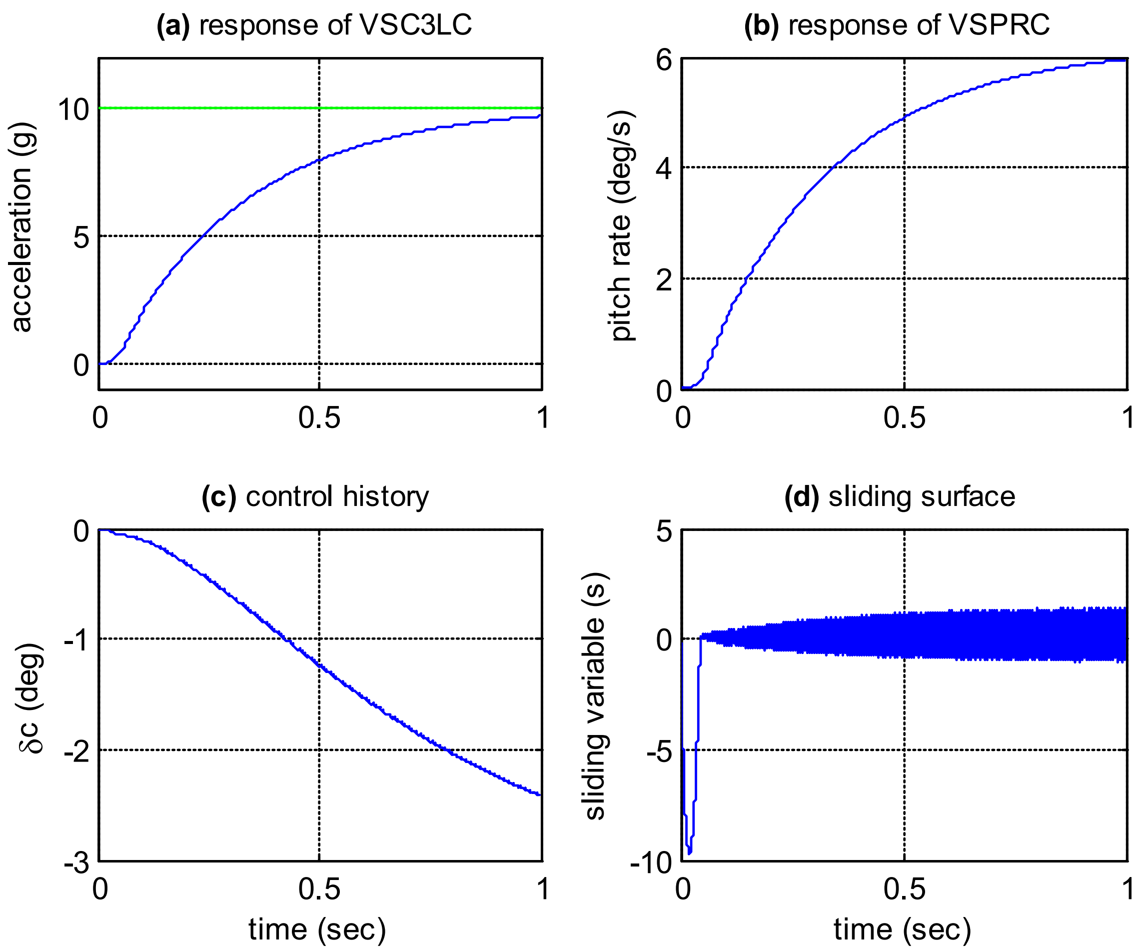

Fig. 6 Responses of VSC3LC and VSPRC with model uncertainties

dynamic coefficients using values of $g_1 = 3594.1$, $g_2 = 84.4$, $g_3 = 8.9$, and $g_4 = 0.4$.

Finally, we compare the performance of VS3LC and VSC3LC using four different admissible uncertainties $\Delta = 0\%, 30\%, 50\%,$ and 70% of the true value. Figure 7 shows the acceleration responses for a command $A_{LC} = 10\ g$. All responses of the proposed variable structure controllers show good asymptotic tracking of the desired acceleration. Figure 7a shows almost identical step responses in the nominal case (without considering the uncertainty). Figure 7b–d shows the classical 3LC which tends to oscillate in the disturbed case, and the difference between the transient response of VS3LC and VSC3LC starts to occur as a result of the unmatched uncertainties. It is seen that the transient performance of VSC3LC is better than the case of VS3LC, because VSPRC, which comprises the inner loop of VSC3LC, is insensitive to unmatched uncertainties.

7 Conclusion

In this study, to achieve robustness against matched and unmatched parametric uncertainties, two feasible designs from a sliding mode control perspective are proposed for longitudinal missile dynamics. The variable structure three-loop controller (VS3LC), which uses the same state feedback as the classical three-loop design when in sliding mode, is presented. Variable structure pitch rate controller (VSPRC), which is insensitive to unmatched as well as matched uncertainties, is derived with expression for uncertainties. The VSPRC combined with an additional outer-loop control results in the proposed VSC3LC which improves the robustness of the classical three-loop design against matched and unmatched uncertainties. The simulation results show acceptable performance regardless of uncertainties. Based on their robust performance, the proposed controllers can be considered as an efficient solution for controlling missile acceleration, subject to parametric variation and un-modeled dynamics.

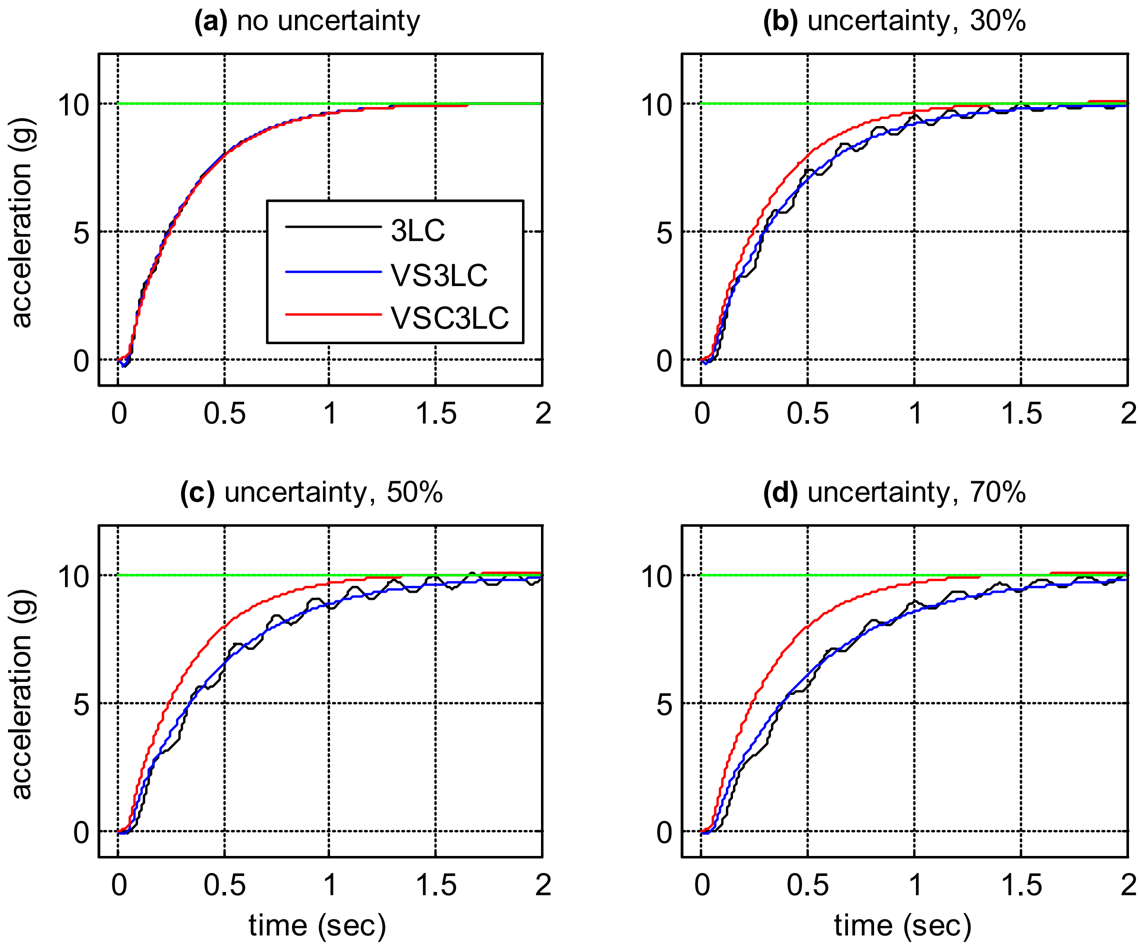

Fig. 7 Comparison of VS3LC, VSC3LC, and 3LC

References

1. Abd-elatif MA, Qian L, Bo Y (2016) Optimization of three-loop missile autopilot gain under crossover frequency constraint. Def Technol 12:32–38
2. Mracek CP, Ridgely DB (2005) Missile longitudinal autopilots: connections between optimal control and classical topologies. AIAA guidance, navigation, and control conference, San Francisco
3. Mracek CP, Ridgely DB (2005) Missile longitudinal autopilots: comparison of multiple three loop topologies. AIAA guidance, navigation, and control conference, San Francisco
4. Xu H, Mirmirani MD, Ioannou PA (2004) Adaptive sliding mode control design for a hypersonic flight vehicle. J Guidance Control Dyn 27(5):829–839
5. Lee Y, Kim Y, Moon G, Jun BE (2014) Boost phase missile attitude controller design using higher-order sliding modes. 29th Congress of the international council of the aeronautical sciences (ICAS 2014), Curran Associates, Inc., Red Hook, NY, pp 3237–3244
6. Shtessel Y, Buffington J, Banda S (2002) Tailless aircraft flight control using multiple time scale reconfigurable sliding modes. IEEE Trans Control Syst Technol 10(2):288–296
7. Lee Y, Kim Y, Moon G, Jun BE (2014) Sliding mode based attitude and acceleration controller for a velocity varying skid to turn missile. 13th European Control Conference (ECC2014), Curran Associates, Inc., Red Hook, NY, pp 2951–2956
8. Idan M, Shima T, Golan OM (2007) Integrated sliding mode autopilot guidance for dual control missiles. J Guidance Control Dyn 30(4):1081–1089
9. Levant A, Pridor A, Gitizadeh R, Yaesh I, Ben-Asher J (2000) Aircraft pitch control via second order sliding technique. J Guidance Control Dyn 23(4):586–594
10. Shtessel YB, Tournes CH (2009) Integrated higher order sliding mode guidance and autopilot for dual control missiles. J Guidance Control Dyn 32(1):79–94
11. Shtessel YB, Shkolnikov IA, Levant A (2007) Smooth second-order sliding modes: missile guidance application. Automatica 43:1470–1476
12. Utkin VI (2013) Sliding modes in control and optimization. Springer, Berlin
13. Zarchan Paul (1997) Tactical and strategic missile guidance. AIAA, Reston, pp 161–180
14. Park KB, Kim SW, Lee JJ (1995) Smooth variable structure controller for robot manipulator using virtual plant. Electron Lett 31(24):2134–2136
15. Tahk MJ, Briggs MM, Menon PK (1988) Application of plant inversion via state feedback to missile autopilot design. In: Proceedings of the 27th Conference on Decision and Control, Austin, Texas, pp 730–735
16. Tahk MJ, Briggs MM (1988) An autopilot design technique based on feedback linearization and wind angle estimation for bank-to-

turn missile systems. In: Proceedings of AIAA Missile sciences conference, Monterey, California
17. Tahk MJ (1990) Robustness characteristics of missile autopilot system based on feedback linearization. JSASS Aircraft Symposium, Tokyo, Japan, pp 360–369
18. Kim SH, Tahk MJ (2011) Missile acceleration controller design using proportional integral and non-linear dynamic control design method. Proc Inst Mech Eng Part G J Aerosp Eng 255(11):882–897